

# Relative contractile motion of the rings in a switchable palindromic [3]rotaxane in aqueous solution driven by radical-pairing interactions

L.S. Witus, K.J. Hartlieb, Y. Wang, A. Prokofjevs, M. Frasconi, J.C. Barnes, E.J. Dale, A.C. Fahrenbach, J.F. Stoddart

## *Supporting Information*

General Methods .....	2
Table S1. References for Compounds Synthesized From Literature Procedures.....	3
Synthesis of Axle A•4PF <sub>6</sub> .....	3
Synthesis of Rotaxanes 2R•8PF <sub>6</sub> and 3R•12PF <sub>6</sub> .....	5
Synthesis of Dumbbell D•4PF <sub>6</sub> .....	7
Figure S1. Cyclic Voltammetry in MeCN .....	8
Figure S2. Spectroelectrochemistry in Aqueous Solution .....	9
Figure S3. UV-Vis-NIR Spectroscopy in MeCN .....	10
Figure S4. UV-Vis-NIR Spectroscopy in Aqueous Solution .....	11
Figure S5. <sup>1</sup> H NMR Spectroscopic Assignment of 3R•12PF <sub>6</sub> .....	12
Figure S6. Low Temperature NMR Spectrum of 3R•12PF <sub>6</sub> .....	13
Figure S7. Variable Temperature NMR Spectra of 3R•12PF <sub>6</sub> .....	14
Figure S8. <sup>1</sup> H- <sup>1</sup> H COSY NMR Spectrum of 3R•12PF <sub>6</sub> .....	15
Figure S9. <sup>1</sup> H- <sup>1</sup> H ROESY NMR Spectrum of 3R•12PF <sub>6</sub> .....	16
Figure S10. <sup>1</sup> H NMR Spectroscopic Assignment of 2R•8PF <sub>6</sub> .....	17
Figure S11. Variable Temperature NMR Spectra of 2R•PF <sub>6</sub> .....	18
Figure S12. <sup>13</sup> C NMR Spectrum of 3R•12PF <sub>6</sub> .....	19
Figure S13. <sup>13</sup> C NMR Spectrum of 2R•8PF <sub>6</sub> .....	20
Figure S14. <sup>1</sup> H NMR Spectrum of D•8PF <sub>6</sub> .....	21
Figure S15. <sup>13</sup> C NMR Spectrum of D•8PF <sub>6</sub> .....	22
Figure S16. <sup>1</sup> H NMR Spectrum of A•8PF <sub>6</sub> .....	23
Figure S17. <sup>13</sup> C NMR Spectrum of A•8PF <sub>6</sub> .....	24
Figure S18. <sup>1</sup> H NMR Spectrum of 3R•12Cl in D <sub>2</sub> O .....	25
Supplemental References.....	26

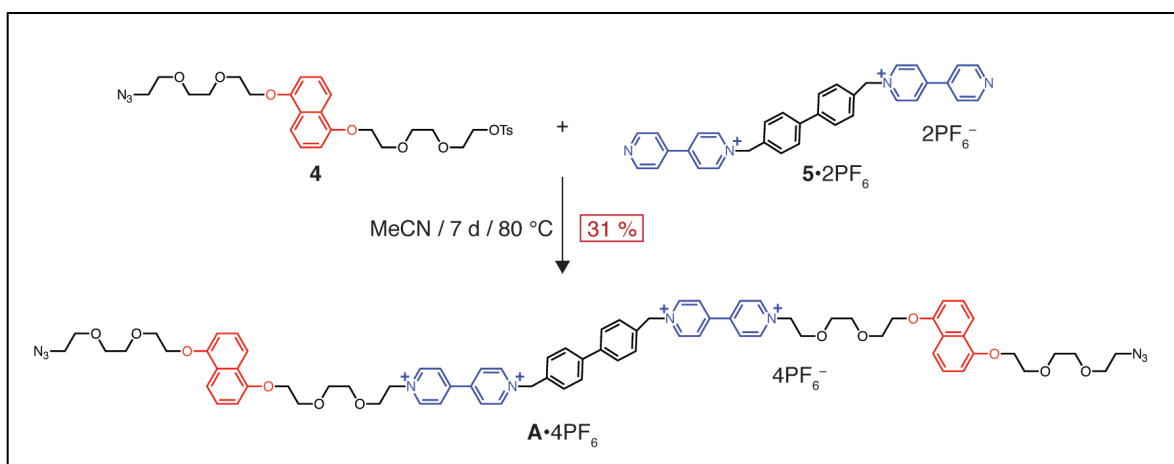
## General Methods

Reagents were purchased from commercial suppliers. The following compounds were prepared according to literature procedures – cyclobis(paraquat-*p*-phenylene) hexafluorophosphate<sup>1</sup> (**CBPQT**·4PF<sub>6</sub>) and compounds 1-6, whose structural formulas are listed in Table S1 along with references to them in the literature. Reverse-phase high-performance liquid chromatography (HPLC) was employed for preparative HPLC purification using a C18-column and a binary solvent system (MeCN and H<sub>2</sub>O with 0.1% CF<sub>3</sub>CO<sub>2</sub>H). A UV-3600 Shimadzu spectrophotometer was used to collect UV-Vis-NIR spectra. Samples for UV-Vis-NIR analysis were prepared at a 0.1 mM concentration in Dulbecco's phosphate-buffered saline or H<sub>2</sub>O. Nuclear magnetic resonance (NMR) spectra were collected on Bruker Avance 500 or 600 spectrometers, with working frequencies of 600 and 500 MHz for <sup>1</sup>H, and 150 and 126 MHz for <sup>13</sup>C nuclei. Chemical shifts are reported in ppm relative to the signals corresponding to the residual non-deuterated solvents (CD<sub>3</sub>CN: δ<sub>H</sub> = 1.94 ppm and δ<sub>C</sub> = 1.32 and 118.26 ppm). An Agilent 6210 Time-of-Flight (TOF) LC-MS, using an ESI source, coupled with Agilent 1100 HPLC mass spectrometer was employed to collect high resolution mass spectra using direct infusion (0.6 mL/min). A Gamry Multipurpose instrument (Reference 600) was used to carry out cyclic voltammetry experiments. These experiments were performed at room temperature in MeCN or Dulbecco's phosphate-buffered saline solutions purged with argon. A glass carbon working electrode (0.071 cm<sup>2</sup>) and a Pt coil counter electrode were used with an Ag/AgCl reference.

Table S1. References for Compounds Synthesized From Literature Procedures.

Compound Number	Structural Formula	Reference
1		<sup>2</sup> S. Fujii and J.-M. Lehn, <i>Angew. Chem. Int. Ed.</i> , 2009, <b>48</b> , 7635–7638.
2		<sup>3</sup> Y. Liu, S. Saha, S. A. Vignon, A. H. Flood, and J. F. Stoddart, <i>Synthesis</i> , 2005, 3437–3445.
3		<sup>4</sup> O. Š. Miljanić, W. R. Dichtel, S. I. Khan, S. Mortezaei, J. R. Heath, and J. F. Stoddart, <i>J. Am. Chem. Soc.</i> , 2007, <b>129</b> , 8236–8246.
4		<sup>2</sup> Y. Liu, S. Saha, S. A. Vignon, A. H. Flood, and J. F. Stoddart, <i>Synthesis</i> , 2005, 3437–3445.
5•2PF <sub>6</sub>		<sup>5</sup> Amabilino, D. B.; Ashton, P. R.; Brown, C. L.; Cordova, E.; Godinez, L. A.; Goodnow, T. T.; Kaifer, A. E.; Newton, S. P.; Pietraszkiwicz, M. <i>J. Am. Chem. Soc.</i> 1995, <b>117</b> , 1271–1293.
6		<sup>6</sup> H. Li, Z. Zhu, A. C. Fahrenbach, B. M. Savoie, C. Ke, J. C. Barnes, J. Lei, Y.-L. Zhao, L. M. Lilley, T. J. Marks, M. A. Ratner, and J. F. Stoddart, <i>J. Am. Chem. Soc.</i> , 2013, <b>135</b> , 456–467.

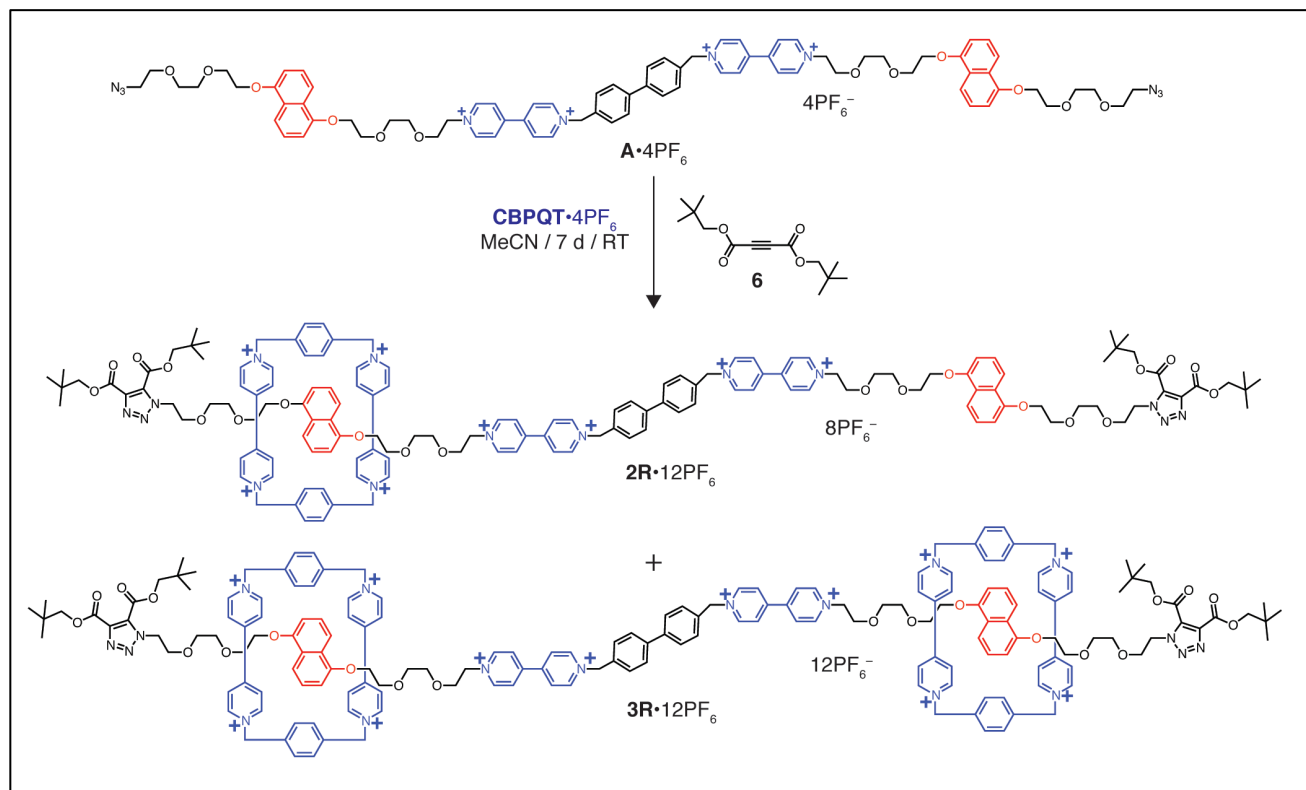
### Synthesis of Axle A•4PF<sub>6</sub>



**A•4PF<sub>6</sub>**: Compounds **4** (500 mg, 0.83 mmol) and **5•2PF<sub>6</sub>** (200 mg, 0.28 mmol) were dissolved in MeCN (10 mL). The reaction mixture was stirred at 80 °C under nitrogen for one week. The

solvent was evaporated and the residue was redissolved in Me<sub>2</sub>CO (4 mL) for purification by silica gel preparative thin layer chromatography (TLC). The preparative TLC plates were run using Me<sub>2</sub>CO with 2% NH<sub>4</sub>PF<sub>6</sub>. The resulting red band was removed from the plate and the silica stirred in Me<sub>2</sub>CO containing 2% NH<sub>4</sub>PF<sub>6</sub> for 15 min. The mixture was filtered, the filtrate collected and the solvent removed in vacuo, resulting in a red solid. The solid was dissolved in a minimal volume of Me<sub>2</sub>CO, H<sub>2</sub>O (100 mL) was added and the precipitate was filtered to remove excess of NH<sub>4</sub>PF<sub>6</sub>, yielding the axle **A**•4PF<sub>6</sub> (148 mg, 31% yield). <sup>1</sup>H NMR (500 MHz, CD<sub>3</sub>CN) δ 8.82 (dd, *J* = 7, 2 Hz, 8H), 7.88 – 7.83 (m, 8H), 7.82 (d, *J* = 7 Hz, 4H), 7.69 (d, *J* = 8 Hz, 4H), 7.38 (d, *J* = 8 Hz, 2H), 7.24 – 7.14 (m, 4H), 7.04 (t, *J* = 9 Hz, 2H), 6.80 (dd, *J* = 23, 8 Hz, 4H), 5.84 (s, 4H), 4.74 – 4.71 (m, 4H), 4.26 – 4.22 (m, 4H), 4.20 – 4.15 (m, 4H), 4.04 – 3.99 (m, 4H), 3.98 – 3.94 (m, 4H), 3.90 – 3.86 (m, 4H), 3.78 – 3.70 (m, 12H), 3.67 – 3.63 (m, 4H), 3.60 – 3.56 (m, 4H), 3.32 – 3.27 (m, 4H). <sup>13</sup>C NMR (126 MHz, CD<sub>3</sub>CN) δ 154.81, 154.64, 149.67, 149.30, 146.70, 145.84, 142.19, 133.35, 131.03, 129.04, 127.27, 126.90, 126.74, 126.62, 126.59, 114.64, 114.38, 106.75, 71.36, 71.03, 70.99, 70.74, 70.39, 70.31, 70.25, 68.98, 68.83, 65.21, 61.98, 51.25. ESI-HRMS calcd for *m/z* = 1791.5509 [*M* – PF<sub>6</sub>]<sup>+</sup>, found *m/z* = 1791.5461.

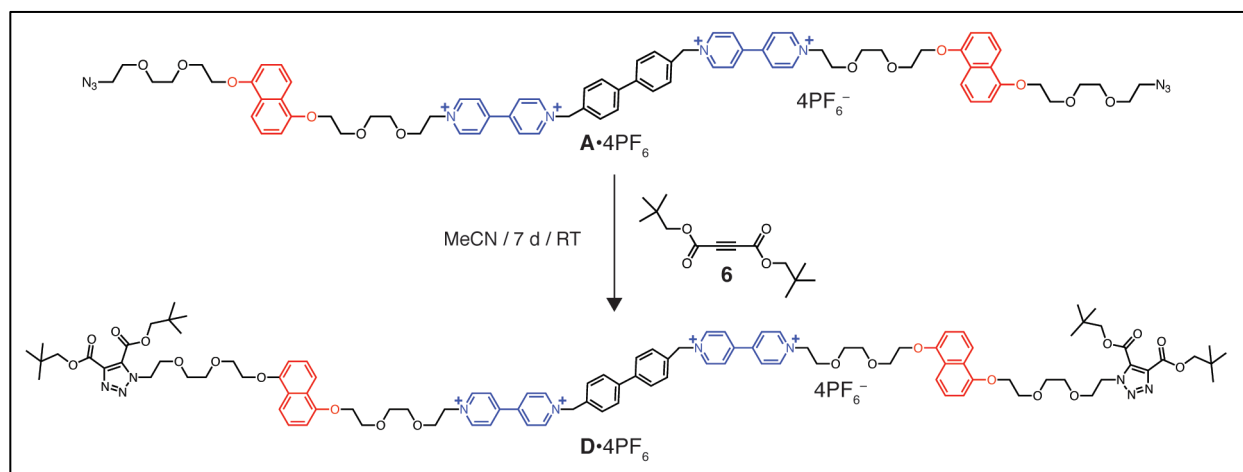
## Synthesis of Rotaxanes $2R \cdot 8PF_6$ and $3R \cdot 12PF_6$



$2R \cdot 8PF_6$  &  $3R \cdot 12PF_6$ : The axle  $A \cdot 4PF_6$  (49 mg, 0.03 mmol) and  $CBPQT \cdot 4PF_6$  (49 mg, 0.03 mmol) were dissolved in MeCN (2 mL), forming a purple solution. Compound **6** (65 mg, 0.26 mmol) was added and the solution stirred at room temperature for 7 d. Addition of tetrabutylammonium chloride resulted in precipitation of a crude mixture, which was filtered off on a fine frit. The resulting solid was purified by reverse-phase HPLC using a gradient of 25 to 50% MeCN in  $H_2O$  containing 0.1% trifluoroacetic acid (TFA). The [3]rotaxane eluted first of all, followed by the [2]rotaxane. Counterion exchange with  $NH_4PF_6$  yielded  $3R \cdot 12PF_6$  (55 mg, 46%) and  $2R \cdot 8PF_6$  (10 mg, 8%), respectively. [2]Rotaxane.  $^1H$  NMR (600 MHz,  $CD_3CN$ )  $\delta$  9.03 – 8.98 (m, 2H), 8.94 – 8.90 (m, 2H), 8.94 – 8.85 (b, 4H), 8.84 (d,  $J = 7$  Hz, 2H), 8.81 (d,  $J = 7$  Hz, 2H), 8.73 – 8.60 (b, 4H), 8.39 (dd,  $J = 7, 2$  Hz, 4H), 7.97 (s, 8H), 7.89 (d,  $J = 7$  Hz, 2H), 7.87 – 7.77 (m, 6H), 7.66 – 7.57 (m, 4H), 7.42 (d,  $J = 8$  Hz, 1H), 7.45 – 7.35 (b, 4H), 7.26 – 7.21 (m, 2H), 7.26 – 7.15 (b, 4H), 7.09 (t,  $J = 9$  Hz, 1H), 6.82 (dd,  $J = 8, 3$  Hz, 2H), 6.30 –

6.20 (m, 2H), 5.97 (dt,  $J = 10$ , 8 Hz, 2H), 5.88 (s, 2H), 5.82 (s, 2H), 5.68 (s, 8H), 4.80 – 4.76 (m, 2H), 4.76 – 4.73 (m, 4H), 4.71 (t,  $J = 6$ , Hz, 2H), 4.35 – 4.31 (m, 2H), 4.27 – 4.22 (m, 4H), 4.23 – 4.19 (m, 4H), 4.17 – 4.14 (m, 4H), 4.12 – 4.09 (m, 4H), 4.08 – 4.01 (m, 12H), 3.99 – 3.96 (m, 4H), 3.94 – 3.89 (m, 10H), 3.88 – 3.83 (m, 4H), 3.78 – 3.71 (m, 4H), 3.67 – 3.63 (m, 2H), 3.59 – 3.55 (m, 2H), 2.44 – 2.37 (m, 2H), 0.97 (s, 9H), 0.96 (s, 9H), 0.94 (s, 9H), 0.91 (s, 9H).  $^{13}\text{C}$  NMR (126 MHz,  $\text{CD}_3\text{CN}$ )  $\delta$  161.37, 161.17, 159.47, 159.45, 154.89, 154.70, 151.88, 151.25, 151.00, 149.76, 147.02, 146.78, 146.56, 146.16, 145.90, 142.20, 142.09, 140.65, 140.59, 137.36, 133.28, 133.21, 132.21, 131.86, 131.52, 131.03, 130.98, 129.06, 129.01, 128.99, 128.94, 128.36, 127.87, 127.35, 126.96, 126.84, 126.78, 126.66, 125.19, 118.49, 114.71, 114.48, 109.18, 109.13, 106.82, 105.27, 105.18, 76.92, 76.75, 75.39, 75.36, 71.72, 71.40, 71.38, 71.16, 71.10, 71.07, 70.79, 70.55, 70.50, 70.37, 70.34, 69.67, 69.60, 69.55, 69.19, 69.03, 68.92, 68.85, 66.08, 65.20, 62.35, 62.05, 51.15, 50.87, 32.10, 32.06, 31.97, 31.94, 26.50, 26.46. ESI-HRMS calcd for  $m/z = 1532.0686 [M - 2(\text{C}_2\text{O}_2\text{F}_3)]^{2+}$ , found  $m/z = 1532.0759$ . [3]Rotaxane.  $^1\text{H}$  NMR (600 MHz,  $\text{CD}_3\text{CN}$ )  $\delta$  9.04 – 8.98 (m, 4H), 8.94 – 8.90 (m, 4H), 8.89 – 8.83 (b, 8H), 8.74 – 8.60 (b, 8H), 8.42 – 8.35 (m, 8H), 8.02 – 7.90 (b, 16H), 7.84 – 7.76 (m, 4H), 7.65 – 7.58 (m, 4H), 7.47 – 7.37 (b, 8H), 7.27 – 7.15 (b, 8H), 6.29 (d,  $J = 8$  Hz, 2H), 6.24 (d,  $J = 8$  Hz, 2H), 5.98 (dt,  $J = 10$ , 8 Hz, 4H), 5.88 (s, 4H), 5.73 – 5.63 (b, 16H), 4.83 – 4.76 (m, 4H), 4.76 – 4.72 (m, 4H), 4.36 – 4.30 (m, 4H), 4.28 – 4.22 (m, 8H), 4.17 – 4.13 (m, 4H), 4.12 – 4.09 (m, 4H), 4.08 – 4.02 (m, 12H), 4.00 – 3.96 (m, 4H), 3.96 – 3.88 (m, 12H), 2.47 – 2.35 (m, 4H), 0.97 (s, 18H), 0.92 (s, 18H).  $^{13}\text{C}$  NMR (126 MHz,  $\text{CD}_3\text{CN}$ )  $\delta$  161.17, 159.45, 151.88, 151.25, 151.01, 147.02, 146.55, 146.17, 145.73, 144.84, 142.11, 140.60, 137.37, 133.18, 132.21, 131.52, 130.98, 129.07, 129.01, 128.94, 128.36, 127.86, 127.33, 127.08, 126.81, 125.69, 125.19, 109.18, 109.13, 105.27, 105.19, 76.91, 75.39, 71.71, 71.41, 71.38, 70.55, 70.50, 69.66, 69.54, 69.19, 69.17, 68.91, 66.07, 65.20, 62.34, 50.87, 32.06, 31.97, 31.96, 26.46. ESI-HRMS calcd for  $m/z = 1308.1193 [M - 3(\text{C}_2\text{O}_2\text{F}_3)]^{3+}$ , found  $m/z = 1308.1204$ .

## Synthesis of Dumbbell D•4PF<sub>6</sub>



**D•4PF<sub>6</sub>:** The axle **A•4PF<sub>6</sub>** (25 mg, 0.01 mmol) was dissolved in MeCN (2 mL), producing a red solution. Compound **6** (33 mg, 0.13 mmol) was added and the solution stirred at room temperature for 7 d. Addition of tetrabutylammonium chloride resulted in precipitation of a crude mixture, which was filtered off on a fine frit. The resulting solid was purified by reverse-phase HPLC using a gradient of 25 to 50% MeCN in H<sub>2</sub>O containing 0.1% TFA. Counterion exchange with NH<sub>4</sub>PF<sub>6</sub> yielded the dumbbell **D•4PF<sub>6</sub>** (10 mg, 31%). <sup>1</sup>H NMR (500 MHz, CD<sub>3</sub>CN) δ 8.82 (dd, *J* = 9, 7 Hz, 8H), 7.88 – 7.78 (m, 12H), 7.65 (d, *J* = 8 Hz, 4H), 7.37 (d, *J* = 8 Hz, 2H), 7.20 (t, *J* = 9 Hz, 2H), 7.12 (d, *J* = 9 Hz, 2H), 7.01 (t, *J* = 9, 2H), 6.82 – 6.73 (m, 4H), 5.80 (s, 4H), 4.73 (t, *J* = 5 Hz, 4H), 4.69 (t, *J* = 6 Hz, 4H), 4.21 – 4.14 (m, 8H), 4.06 – 4.00 (m, 8 H), 3.98 (s, 4H), 3.91 – 3.81 (m, 12H), 3.78 – 3.70 (m, 8H), 3.68 – 3.63 (m, 4H), 3.59 – 3.54 (m, 4H), 0.94 (s, 18H), 0.92 (s, 18H). <sup>13</sup>C NMR (126 MHz, CD<sub>3</sub>CN) δ 161.34, 159.45, 154.83, 154.64, 149.68, 149.29, 146.75, 145.87, 142.19, 140.65, 133.35, 131.83, 131.03, 129.07, 127.33, 126.93, 126.80, 126.74, 126.63, 114.67, 114.41, 106.77, 76.73, 75.34, 71.15, 71.09, 71.04, 70.77, 70.34, 69.58, 69.01, 68.87, 68.80, 65.23, 62.01, 51.12, 32.08, 31.93. ESI-HRMS calcd for *m/z* = 1045.9672 [*M* – 2(C<sub>2</sub>O<sub>2</sub>F<sub>3</sub>)]<sup>2+</sup>, found *m/z* = 1045.9685.

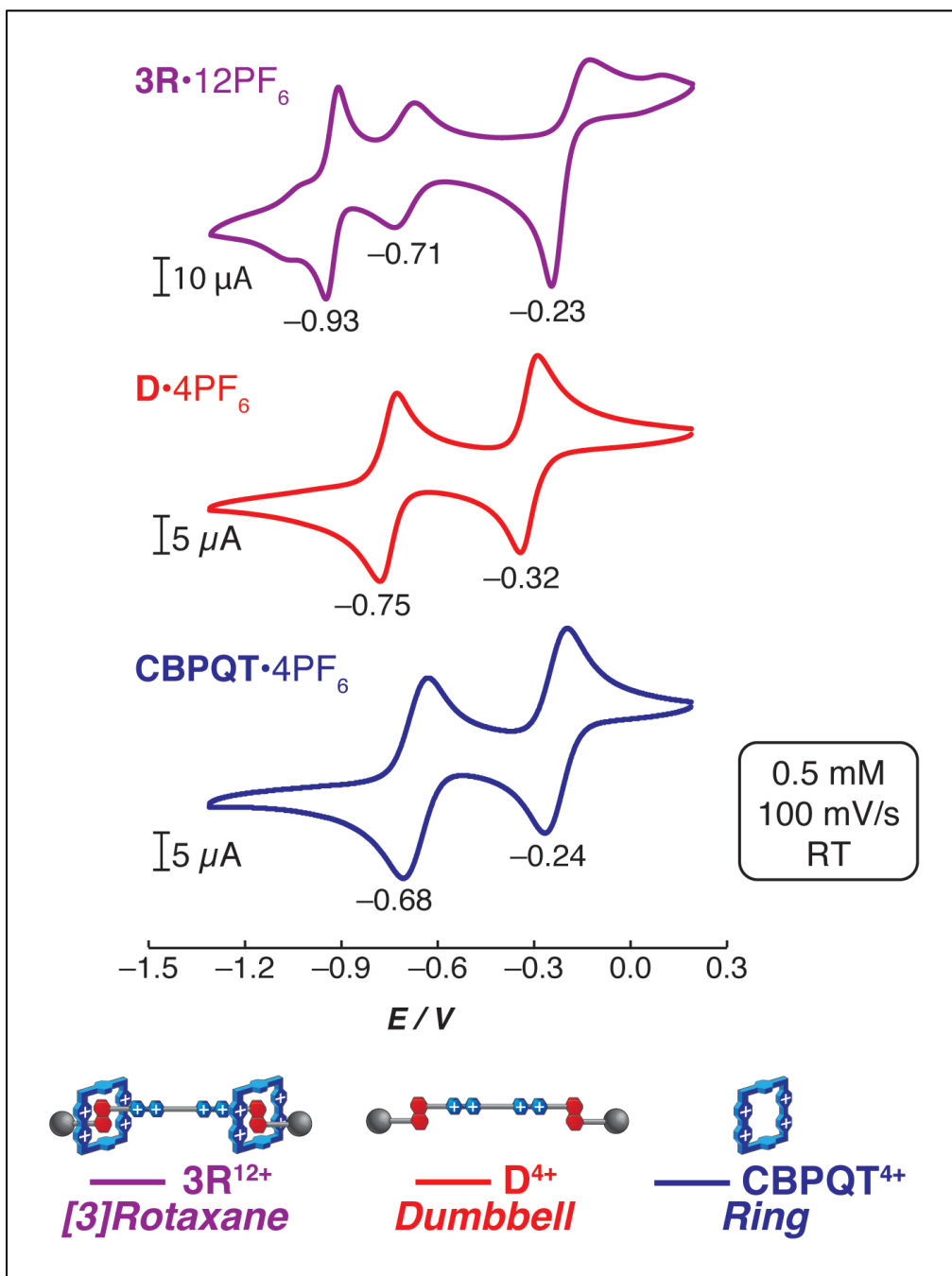


**Figure S1. Cyclic Voltammetry in MeCN**

Cyclic voltammetry (CV) was performed on **3R•12PF<sub>6</sub>**, **D•4PF<sub>6</sub>**, and **CBPQT•4PF<sub>6</sub>** in MeCN.

The CVs were recorded at room temperature in argon-purged solutions using a concentration of 0.5 mM sample and 0.1 mM electrolyte (tetrabutylammonium hexafluorophosphate). The scan

rate was set at 100 mV/s. In the case of the [3]rotaxane, three reduction peaks were observed, a situation that corresponds to a total of a 12-electron reduction from the fully oxidized to the neutral species.

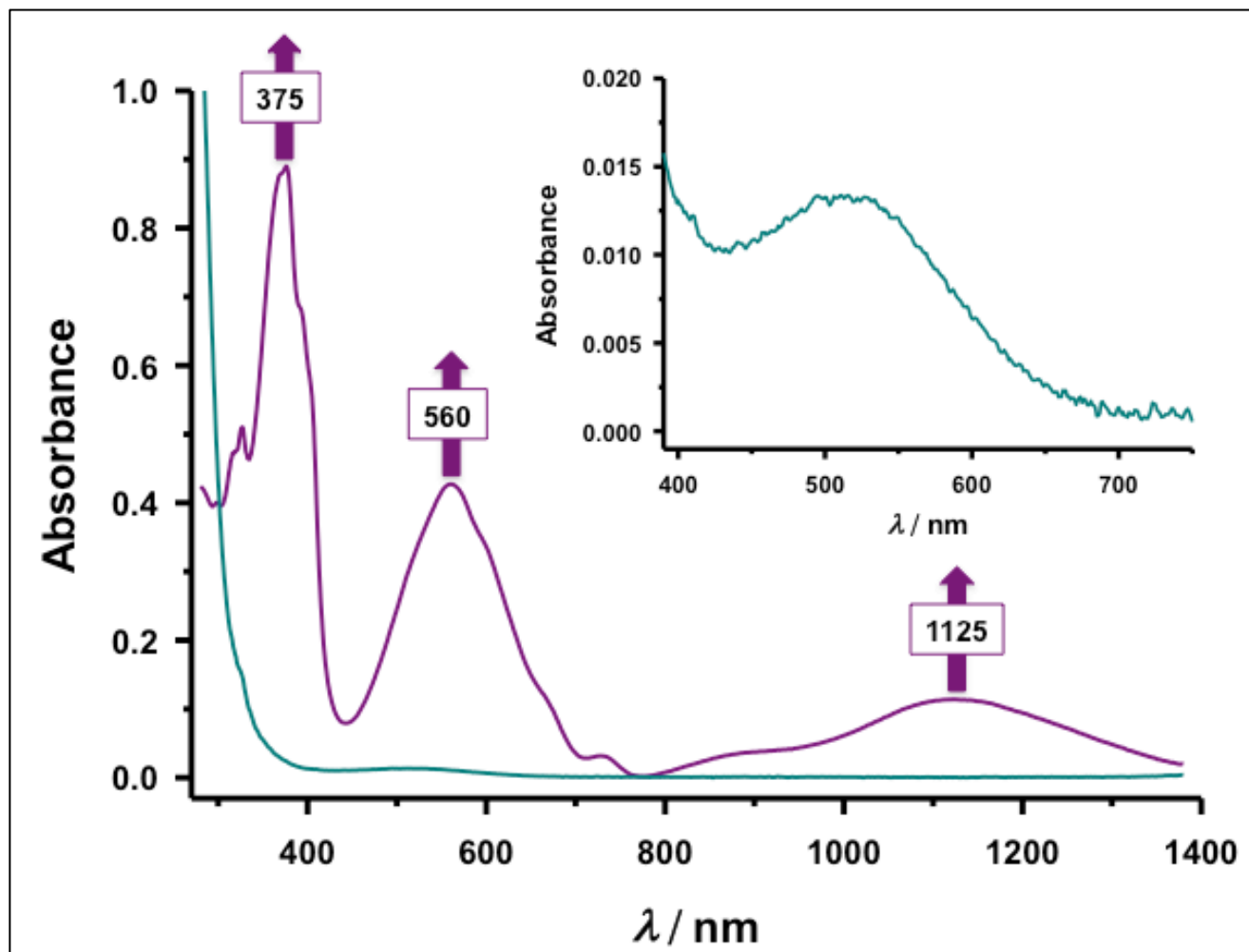


**Figure S2. Spectroelectrochemistry in Aqueous Solution**

UV-Vis spectra of [3]rotaxane  $3R \cdot 12Cl$  (60  $\mu M$ ) conducted at 298 K in  $H_2O/DMF$  90/10 (v/v) ( $KNO_3$  0.1 M) before (green curve) and after (purple curve) applying a potential of  $-0.75 V$  vs  $Ag/AgCl$  *Inset*. Close-up view of the charge transfer adsorption band of the green curve.

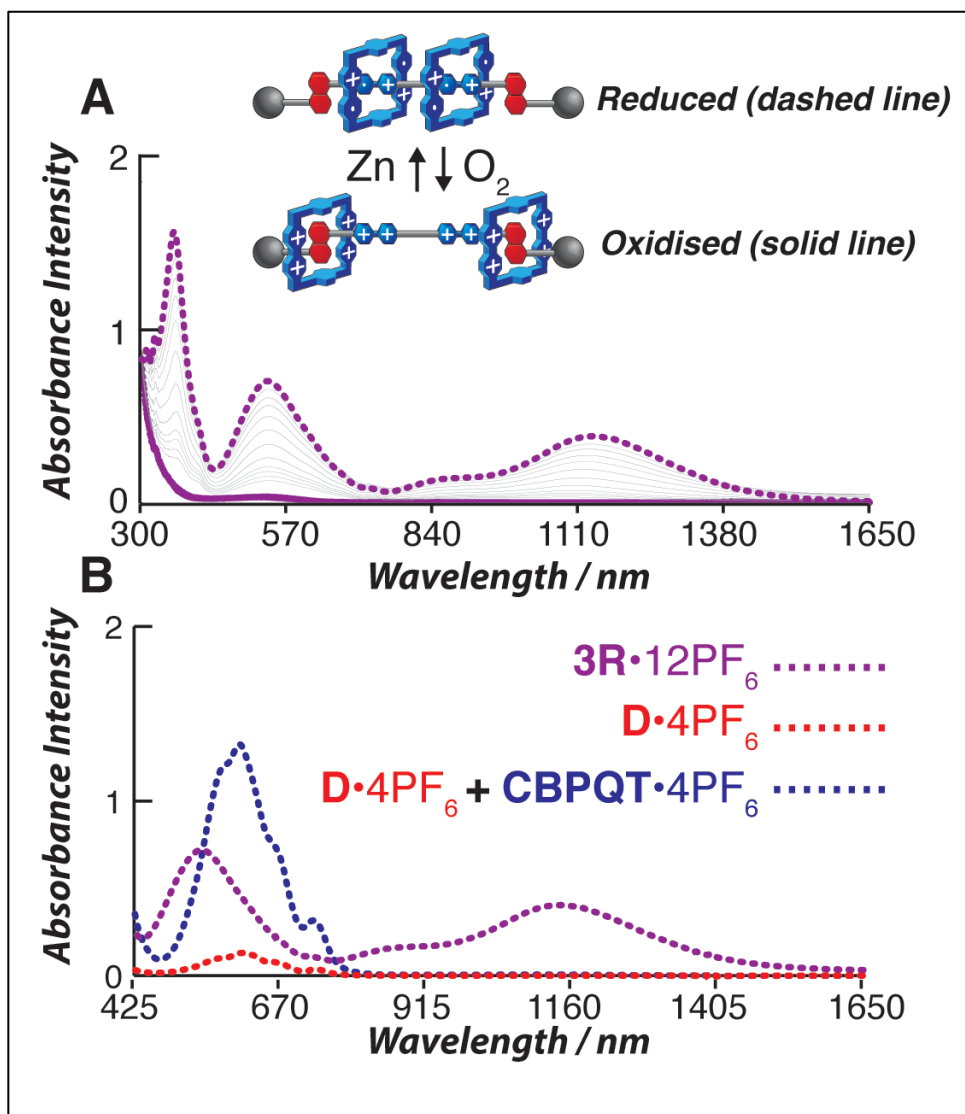


**Figure S3. UV-Vis-NIR Spectroscopy in MeCN**

UV-Vis-NIR Spectra in MeCN (0.1 mM sample). **A**) Zinc dust and O<sub>2</sub> were used to convert between the reduced (dashed lines) and oxidised (solid lines) forms of the [3]rotaxane **3R**•12PF<sub>6</sub>. **B**) A comparison of the absorptions of the reduced forms of the dumbbell and [3]rotaxane. As a control, a solution of a 1:1 mixture of the dumbbell and the ring was also prepared. Compared to the [3]rotaxane, the NIR absorbance resulting from the radical-radical pairing interaction, was not observed when the components were not mechanically interlocked.

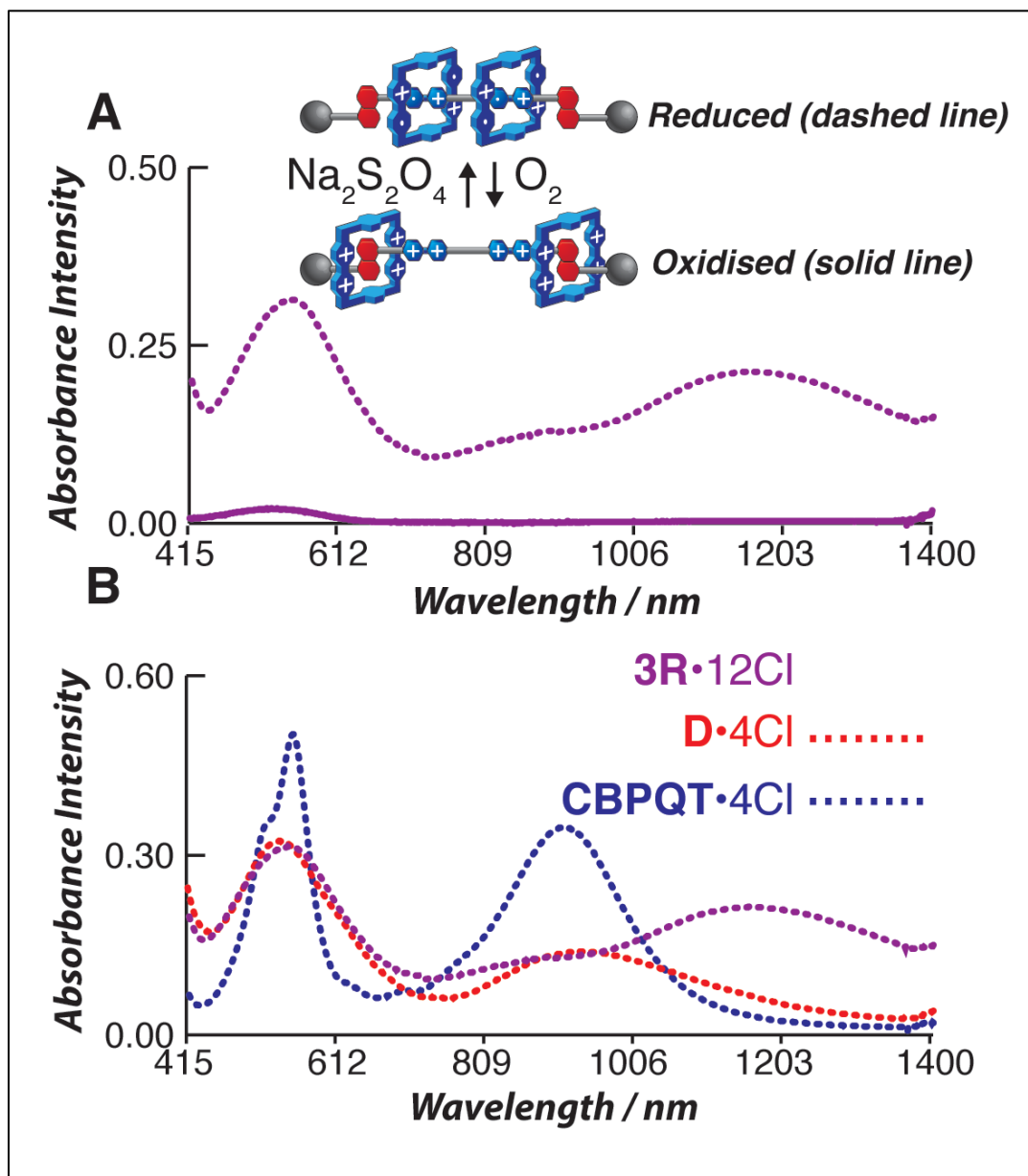


**Figure S4. UV-Vis-NIR Spectroscopy in Aqueous Solution**

UV-Vis-NIR Spectra in phosphate buffered saline (0.1 mM sample). A)  $\text{Na}_2\text{S}_2\text{O}_4$  and  $\text{O}_2$  were used to switch between the reduced (dashed lines) and oxidised (solid lines) forms of the [3]rotaxane, **3R•12Cl**. B) A comparison of the absorption spectra of the reduced forms of the dumbbell, ring and [3]rotaxane.

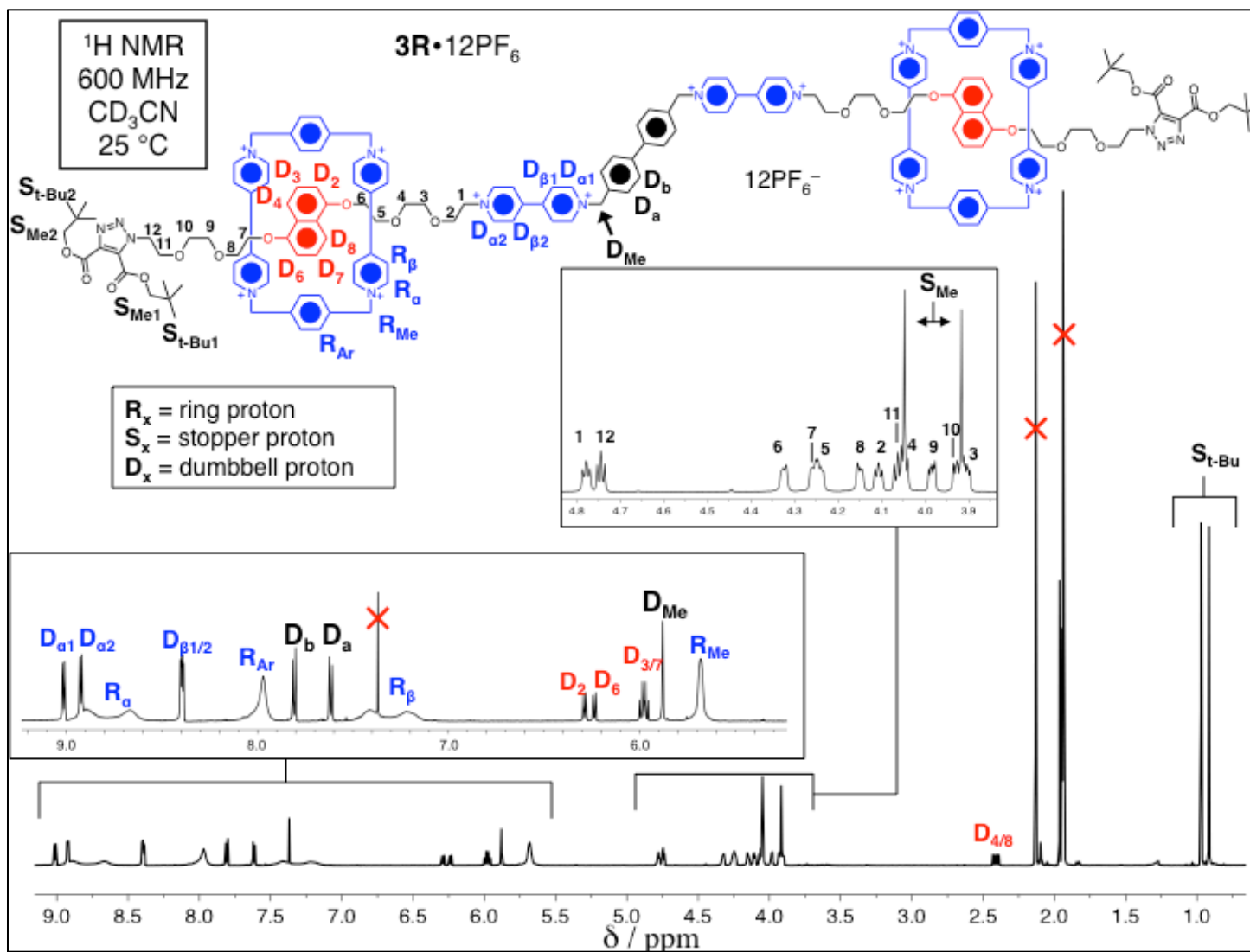


**Figure S5. <sup>1</sup>H NMR Spectroscopic Assignment of 3R•12PF<sub>6</sub>**

<sup>1</sup>H NMR Spectrum (600 MHz) of 3R•12PF<sub>6</sub> in CD<sub>3</sub>CN at 25 °C.

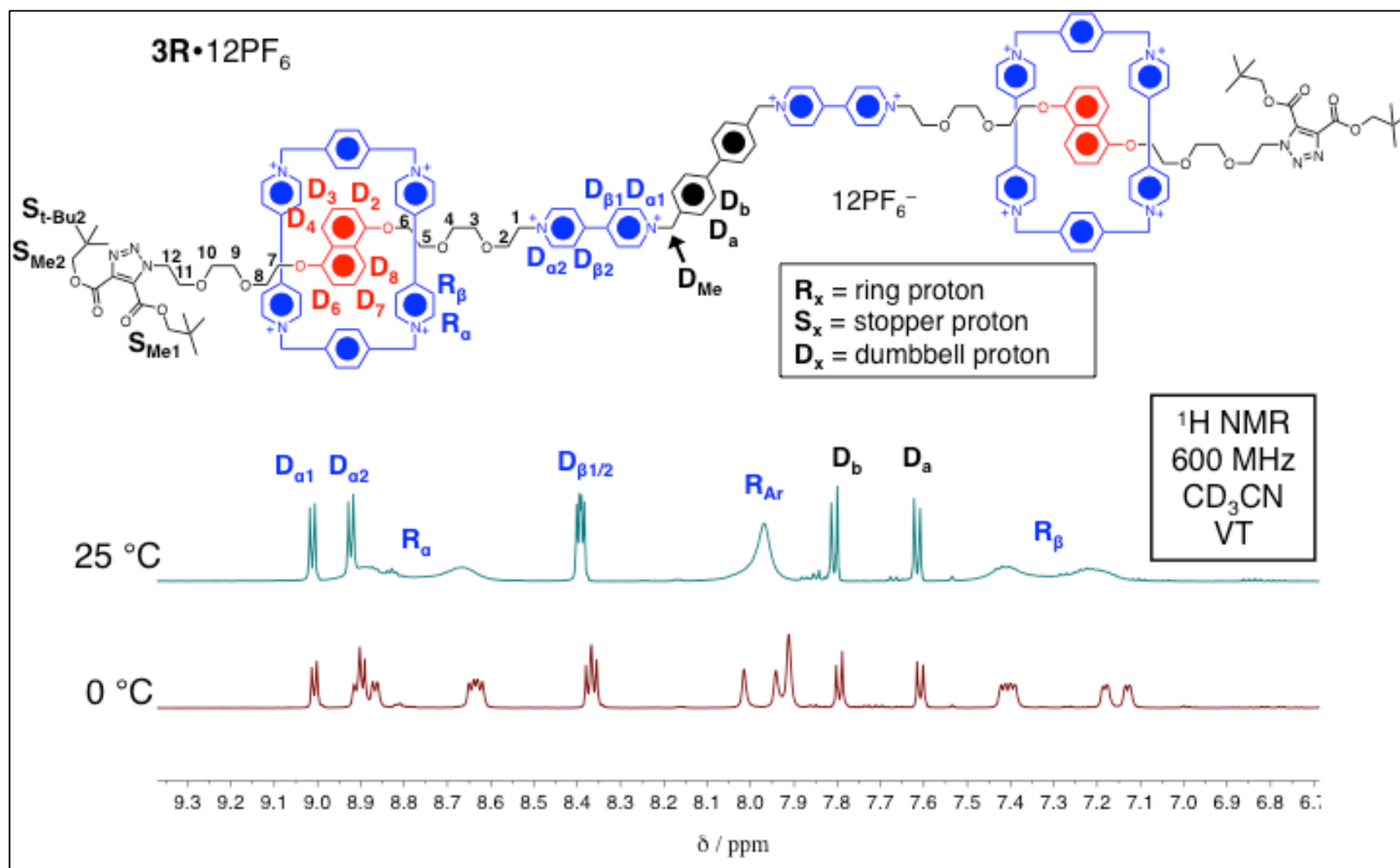


**Figure S6. Low Temperature NMR Spectrum of 3R•12PF<sub>6</sub>**

<sup>1</sup>H NMR Spectrum (600 MHz) of **3R•12PF<sub>6</sub>** in CD<sub>3</sub>CN at 25 °C and 0 °C. The peaks for the ring protons were resolved at the lower temperature.

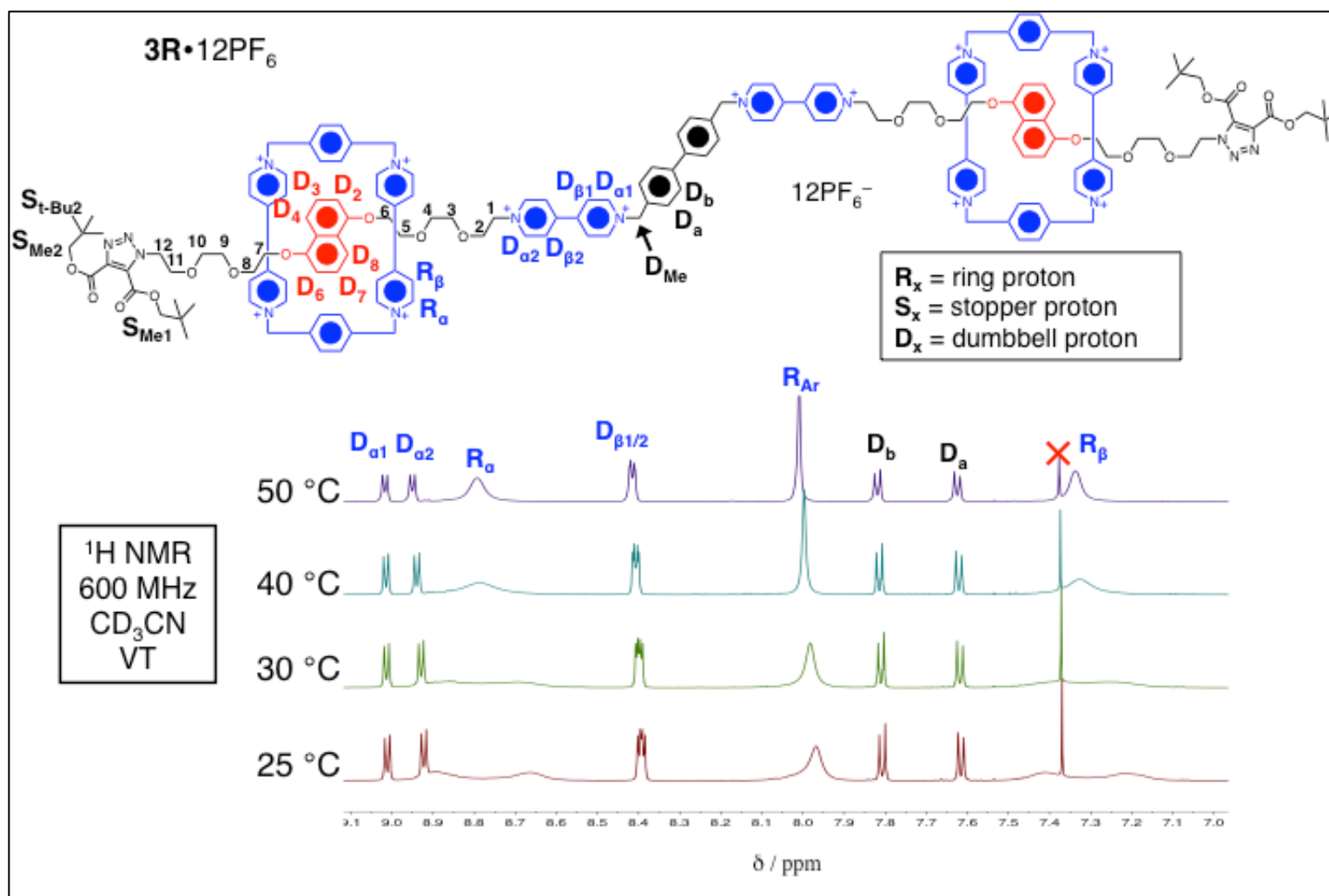


**Figure S7. Variable Temperature NMR Spectra of 3R•12PF<sub>6</sub>**

<sup>1</sup>H NMR Spectrum (600 MHz) of 3R•12PF<sub>6</sub> in CD<sub>3</sub>CN at 25 °C through 50 °C. The peaks for the ring protons coalesced at the higher temperatures.

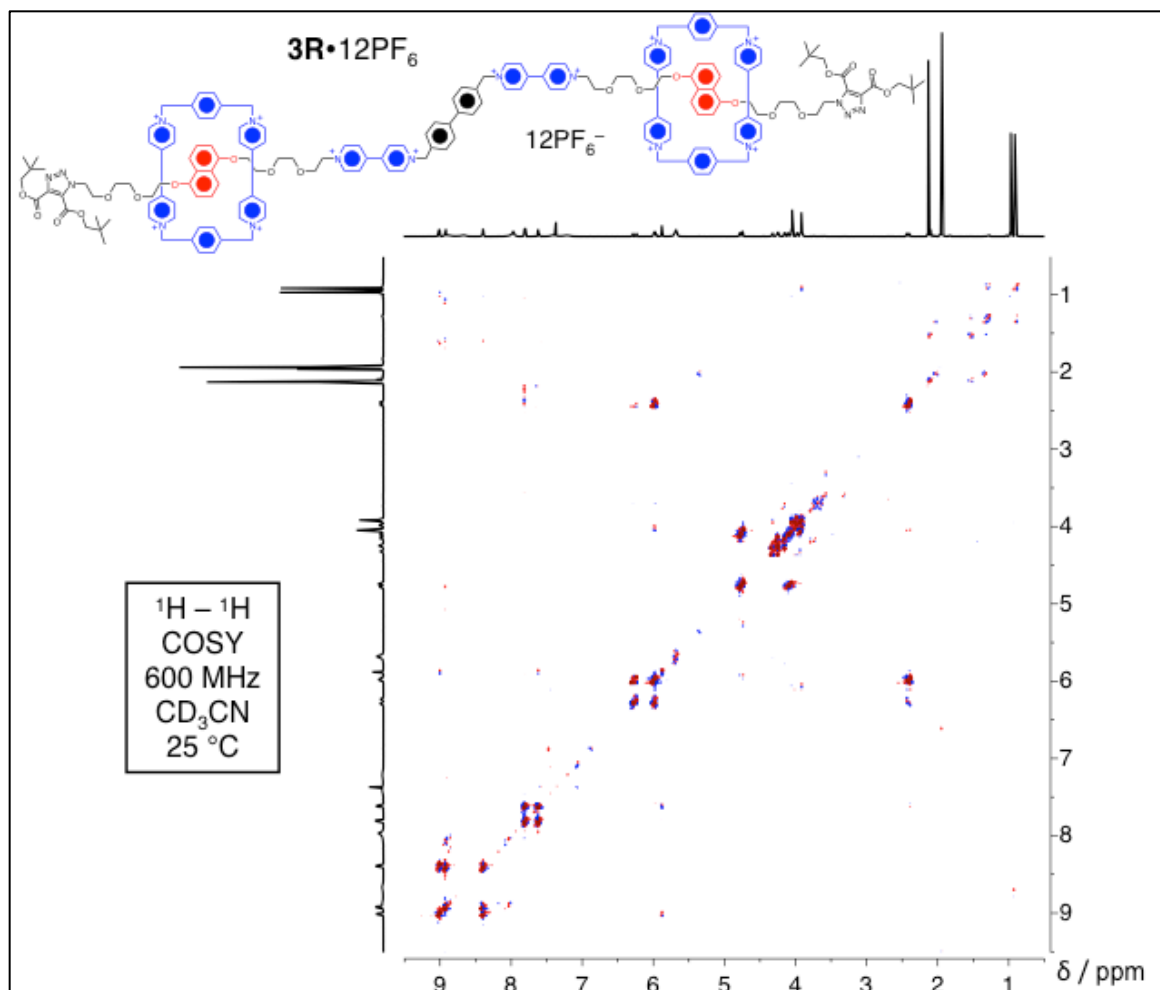


**Figure S8.**  $^1H$ - $^1H$  COSY NMR Spectrum of  $3R \cdot 12PF_6$

$^1H$ - $^1H$  Gradient-selected double-quantum filtered phase-sensitive COSY NMR spectrum (600 MHz, pulse width of 9.5) of  $3R \cdot 12PF_6$  in  $CD_3CN$  at 25 °C.

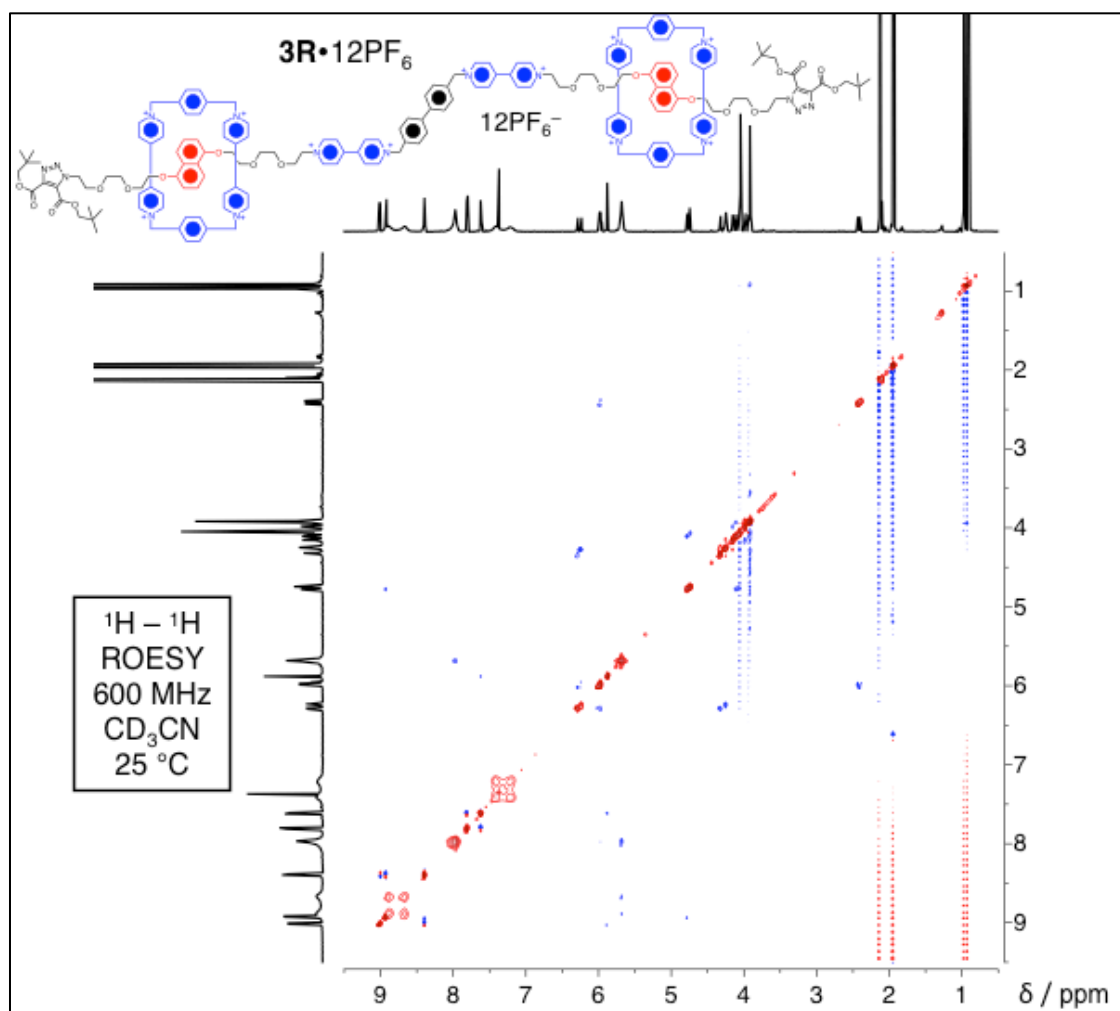
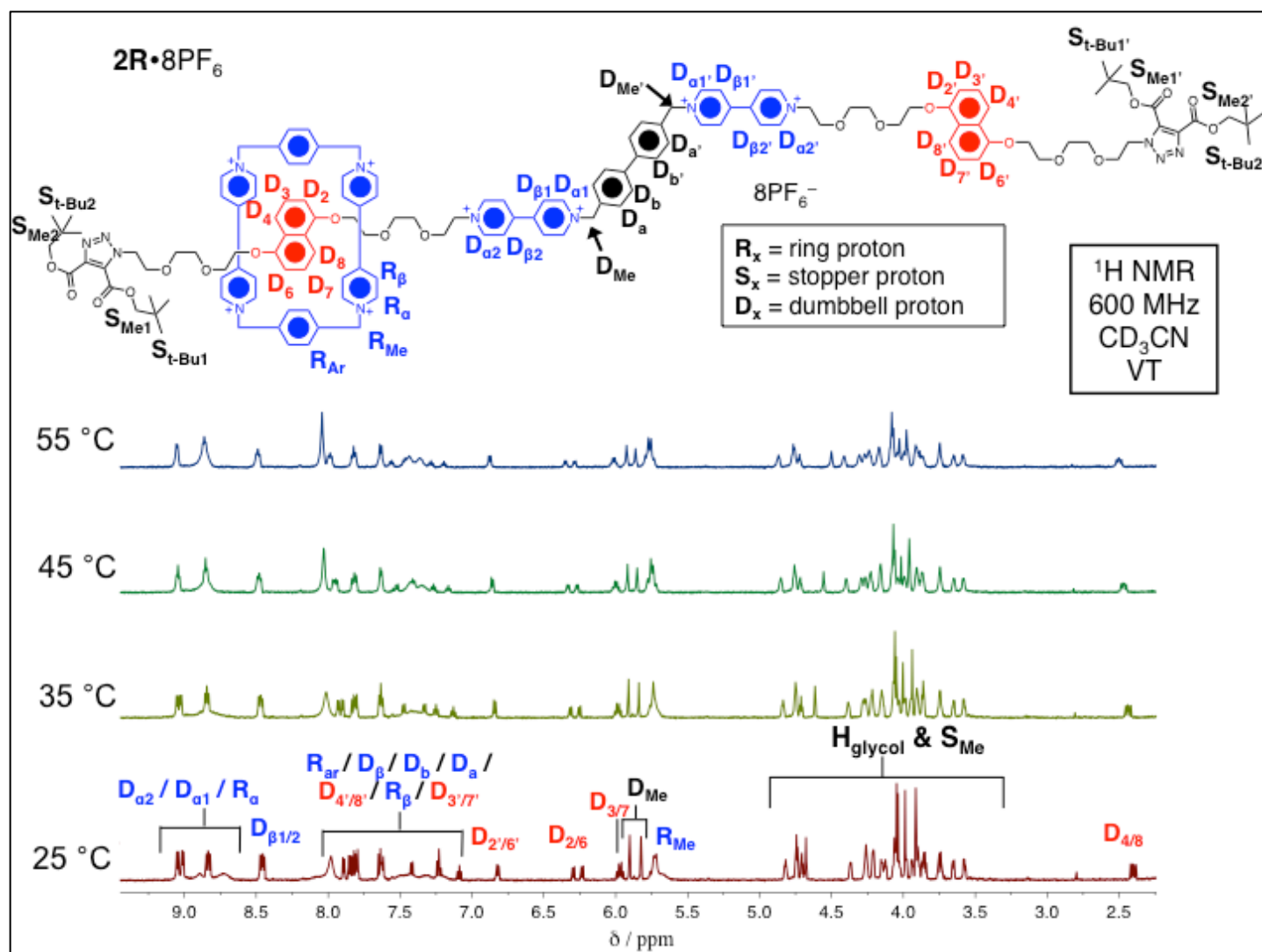


Figure S9.  $^1\text{H}$ - $^1\text{H}$  ROESY NMR Spectrum of  $3\text{R}\cdot 12\text{PF}_6$

$^1\text{H}$ - $^1\text{H}$  ROESY NMR Spectrum (600 MHz, pulse width of 9.5, mixing time of 0.7 s determined by inversion recovery experiment) of  $3\text{R}\cdot 12\text{PF}_6$  in  $\text{CD}_3\text{CN}$  at 25 °C.





**Figure S11. Variable Temperature NMR Spectra of 2R•PF<sub>6</sub>**

<sup>1</sup>H NMR Spectrum (600 MHz) of **2R•8PF<sub>6</sub>** in CD<sub>3</sub>CN at 25 °C through 55 °C.

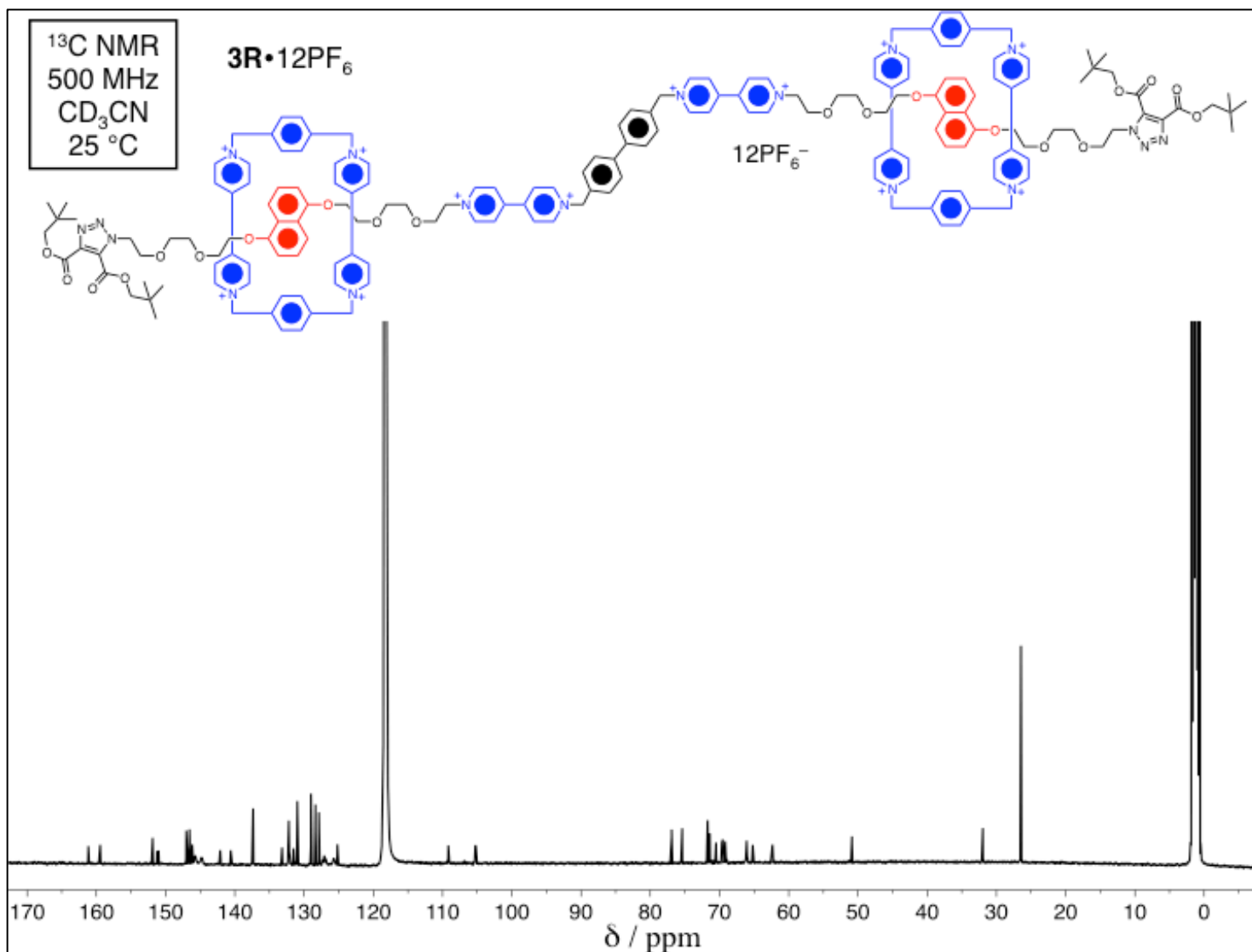


**Figure S12.**  $^{13}\text{C}$  NMR Spectrum of **3R•12PF<sub>6</sub>**

$^{13}\text{C}$  NMR Spectrum (500 MHz) of **3R•12PF<sub>6</sub>** in  $\text{CD}_3\text{CN}$  at 25 °C.

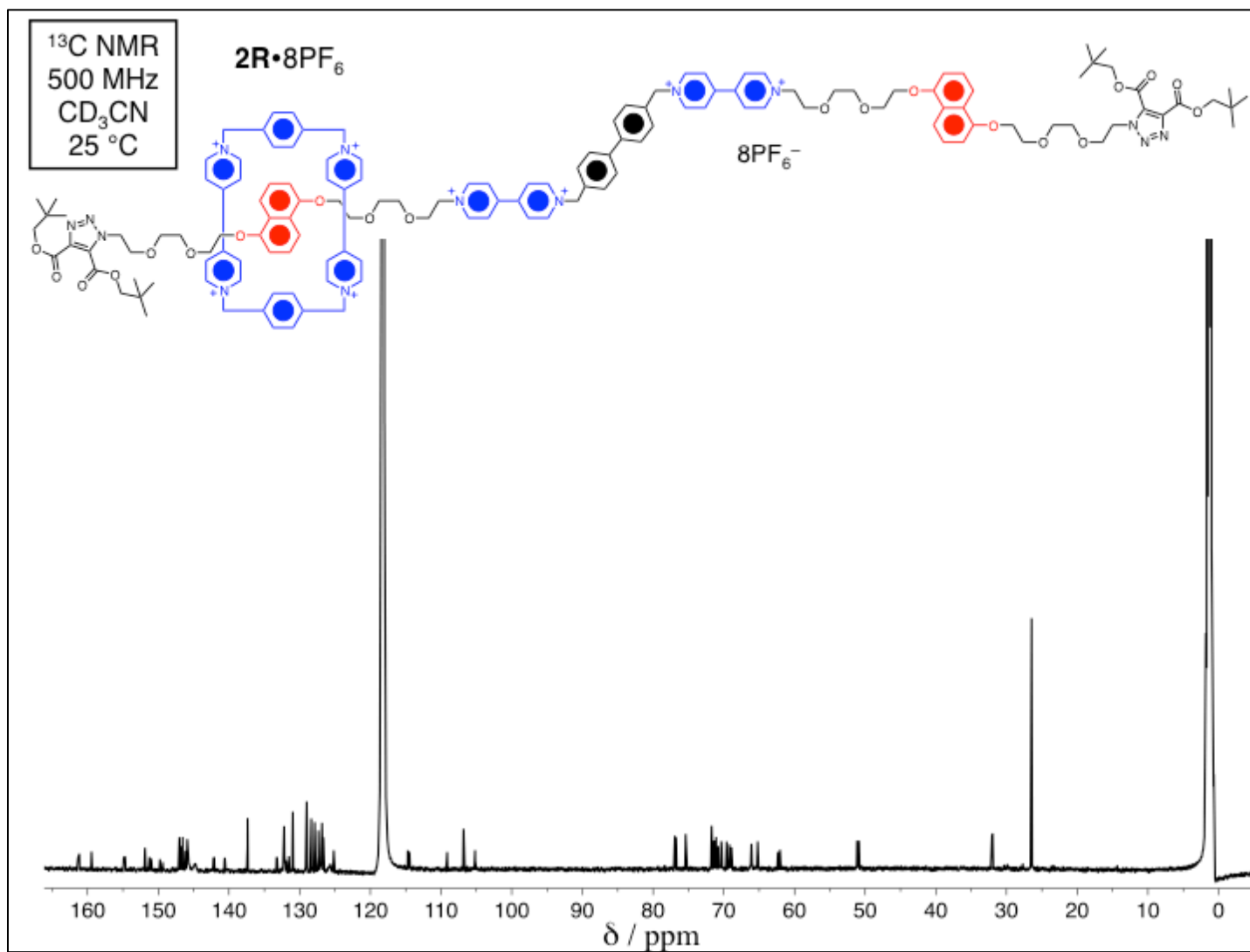


**Figure S13.**  $^{13}\text{C}$  NMR Spectrum of **2R**• $8\text{PF}_6^-$

$^{13}\text{C}$  NMR Spectrum (500 MHz) of **2R**• $8\text{PF}_6^-$  in  $\text{CD}_3\text{CN}$  at 25 °C.

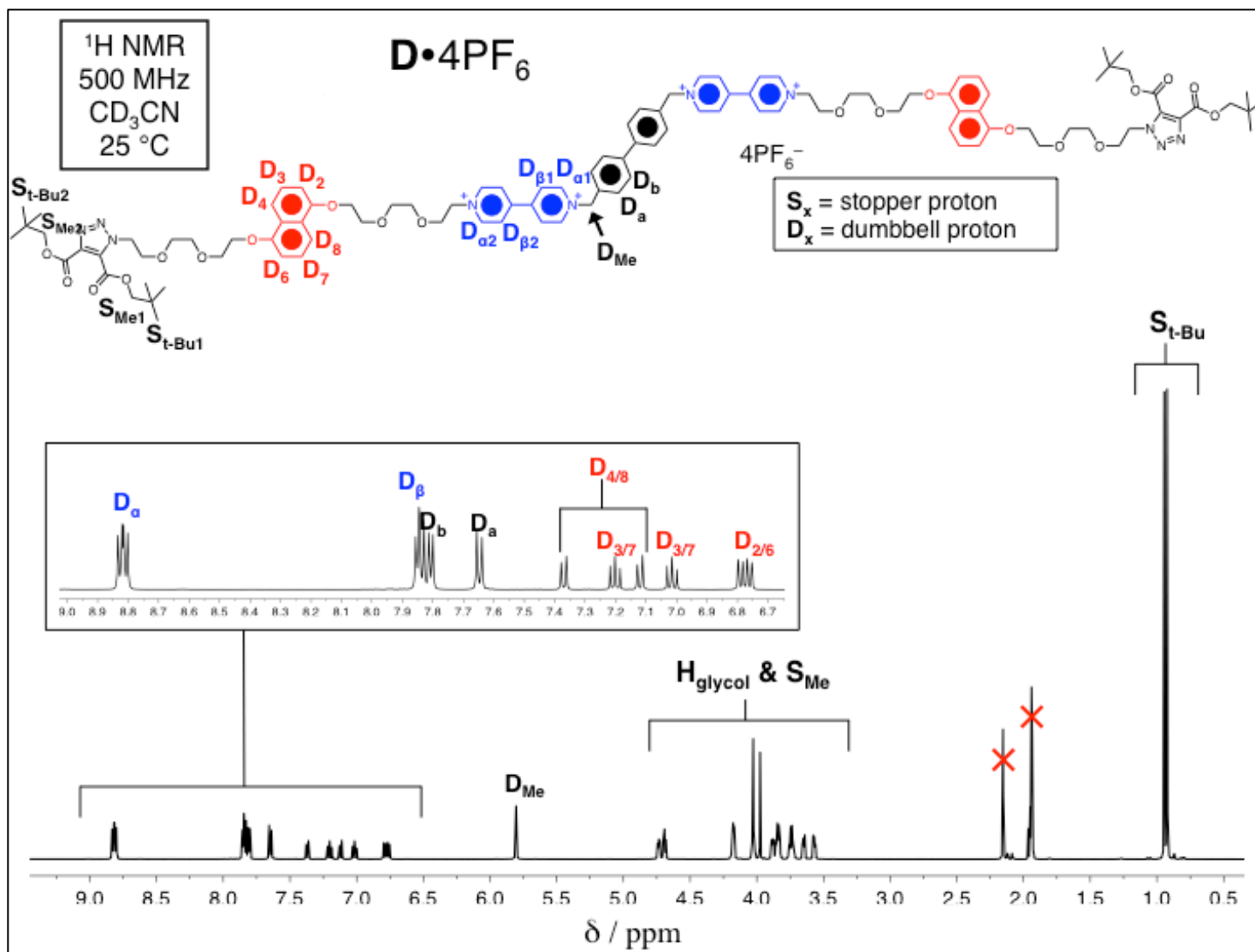


**Figure S14.  $^1\text{H}$  NMR Spectrum of  $\text{D}\cdot 8\text{PF}_6$**

$^1\text{H}$  NMR Spectrum (500 MHz) of  $\text{D}\cdot 8\text{PF}_6$  in  $\text{CD}_3\text{CN}$  at 25 °C.

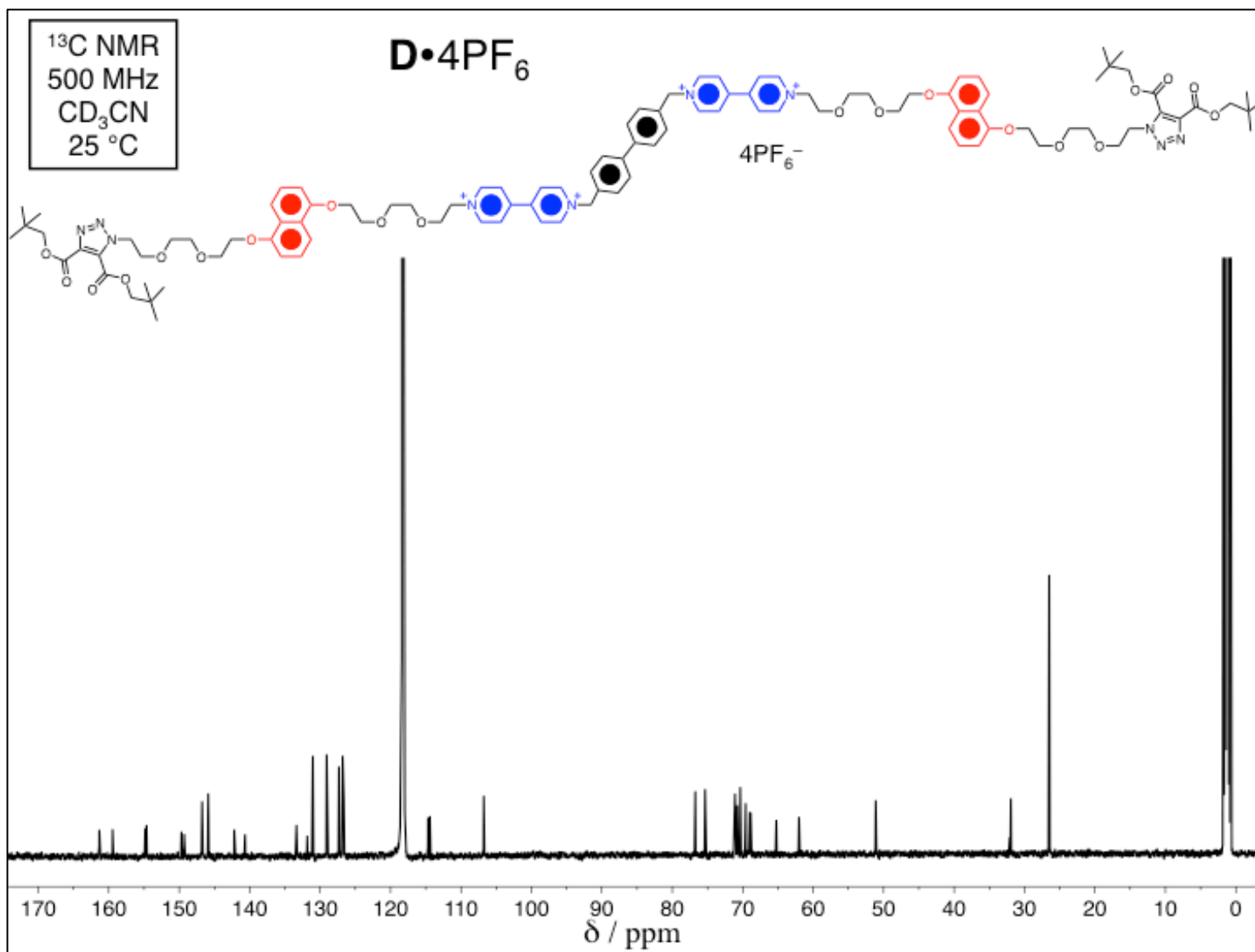


**Figure S15.** <sup>13</sup>C NMR Spectrum of **D•8PF<sub>6</sub>**

<sup>13</sup>C NMR Spectrum (500 MHz) of **D•8PF<sub>6</sub>** in CD<sub>3</sub>CN at 25 °C.

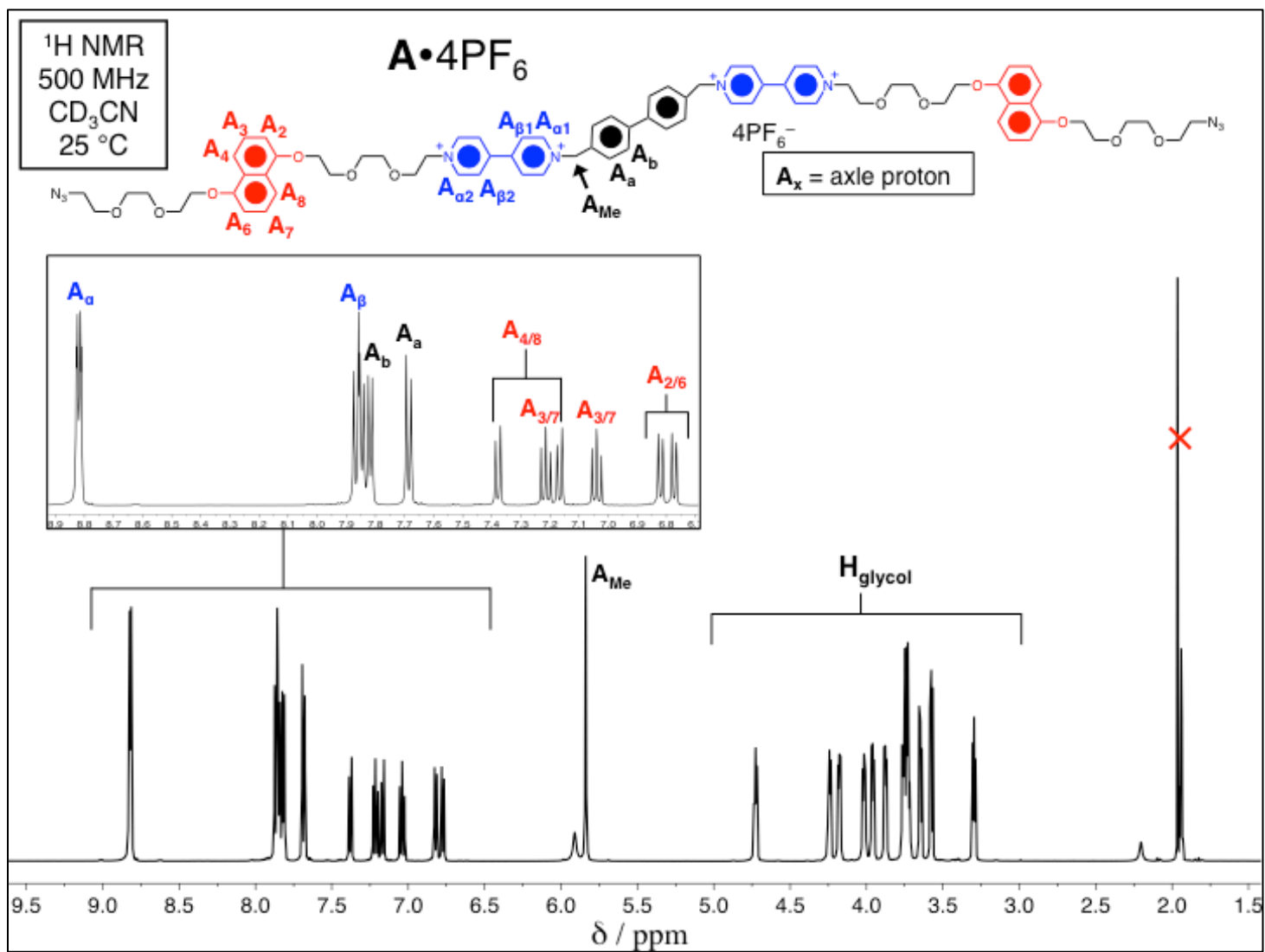


**Figure S16.  ${}^1\text{H}$  NMR Spectrum of  $\mathbf{A} \cdot 8\text{PF}_6$**

${}^1\text{H}$  NMR Spectrum (500 MHz) of  $\mathbf{A} \cdot 8\text{PF}_6$  in  $\text{CD}_3\text{CN}$  at 25 °C.

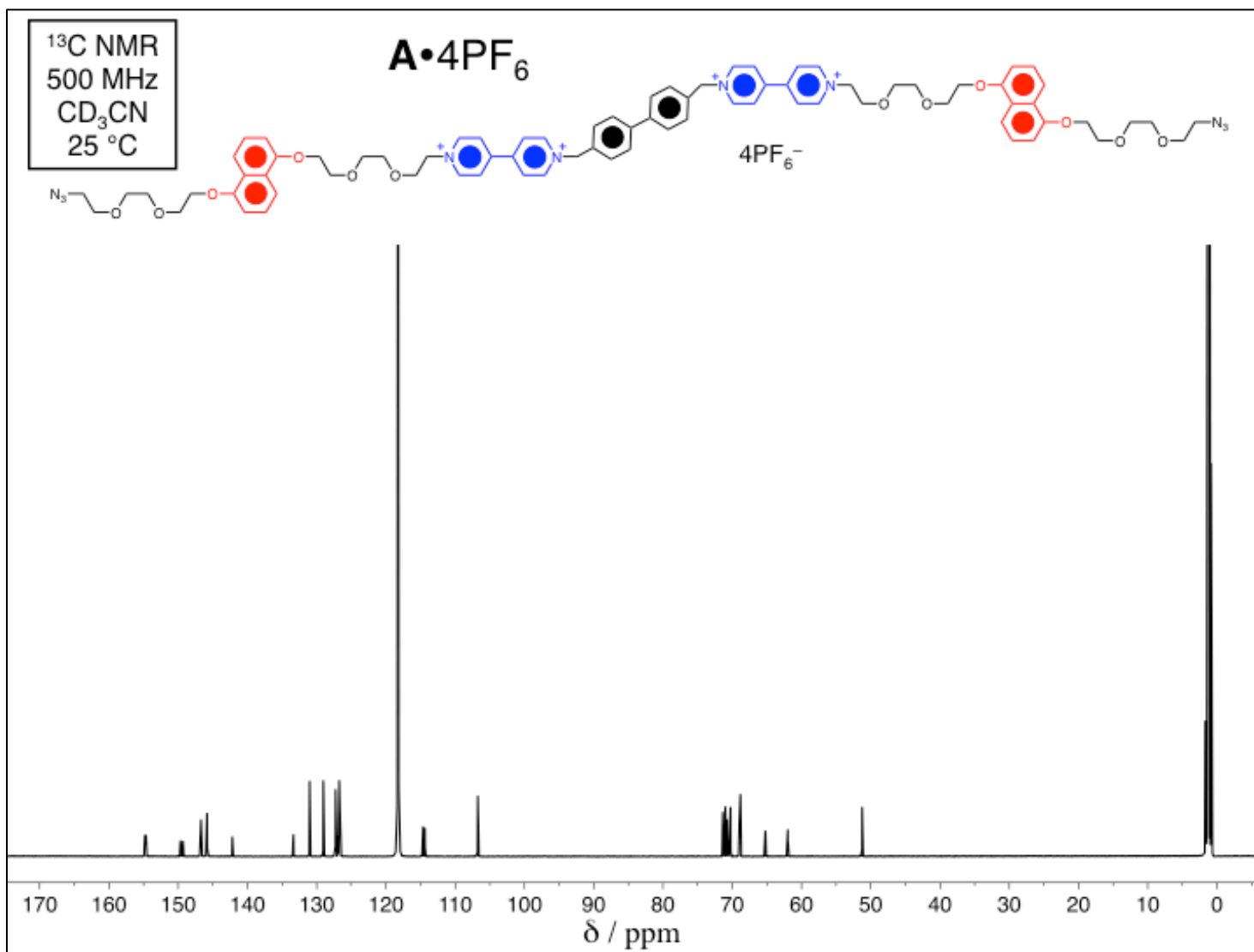


**Figure S17.  $^{13}\text{C}$  NMR Spectrum of  $\text{A}\cdot 8\text{PF}_6$**

$^{13}\text{C}$  NMR Spectrum (500 MHz) of  $\text{A}\cdot 8\text{PF}_6$  in  $\text{CD}_3\text{CN}$  at 25 °C.

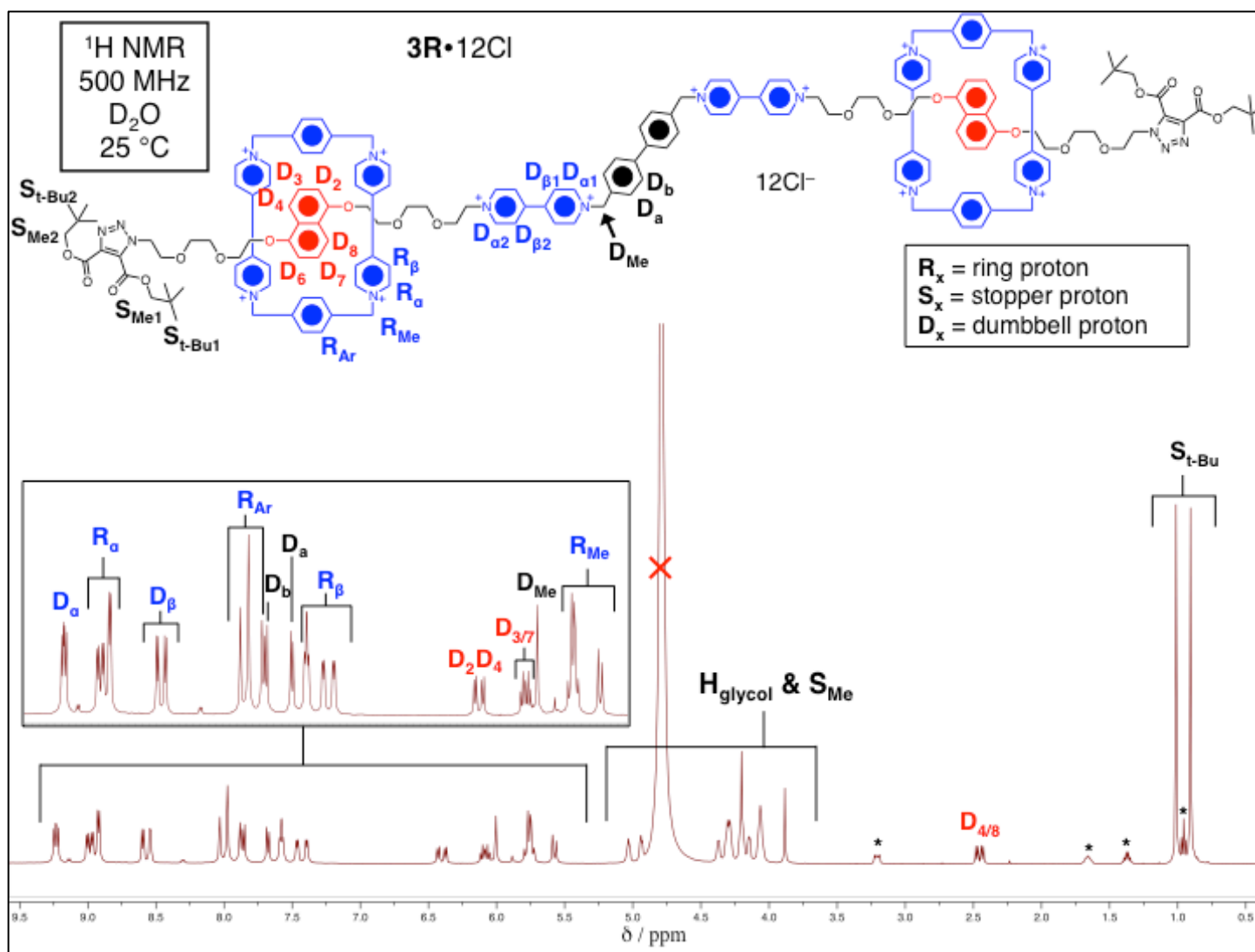


**Figure S18.  $^1\text{H NMR}$  Spectrum of  $3\text{R}\cdot 12\text{Cl}$  in  $\text{D}_2\text{O}$**

$^1\text{H NMR}$  Spectrum (500 MHz) of  $3\text{R}\cdot 12\text{Cl}$  in  $\text{D}_2\text{O}$  at 25 °C.

## Supplemental References

- <sup>1</sup> M. Asakawa, W. Dehaen, G. L'abbé, S. Menzer, J. Nouwen, F. M. Raymo, J. F. Stoddart, and D. J. Williams, *J. Org. Chem.*, 1996, **61**, 9591–9595.
- <sup>2</sup> S. Fujii and J.-M. Lehn, *Angew. Chem. Int. Ed.*, 2009, **48**, 7635–7638.
- <sup>3</sup> Y. Liu, S. Saha, S. A. Vignon, A. H. Flood, and J. F. Stoddart, *Synthesis*, 2005, 3437–3445.
- <sup>4</sup> O. Š. Miljanić, W. R. Dichtel, S. I. Khan, S. Mortezaei, J. R. Heath, and J. F. Stoddart, *J. Am. Chem. Soc.*, 2007, **129**, 8236–8246.
- <sup>5</sup> Amabilino, D. B.; Ashton, P. R.; Brown, C. L.; Cordova, E.; Godinez, L. A.; Goodnow, T. T.; Kaifer, A. E.; Newton, S. P.; Pietraszkiewicz, M. *J. Am. Chem. Soc.* 1995, **117**, 1271–1293.
- <sup>6</sup> H. Li, Z. Zhu, A. C. Fahrenbach, B. M. Savoie, C. Ke, J. C. Barnes, J. Lei, Y.-L. Zhao, L. M. Lilley, T. J. Marks, M. A. Ratner, and J. F. Stoddart, *J. Am. Chem. Soc.*, 2013, **135**, 456–467.
- <sup>7</sup> H. Li, A. C. Fahrenbach, A. Coskun, Z. Zhu, G. Barin, Y.-L. Zhao, Y. Y. Botros, J.-P. Sauvage, and J. F. Stoddart, *Angew. Chem. Int. Ed.*, 2011, **50**, 6782–6788 and H. Li, Y.-L. Zhao, A. C. Fahrenbach, S.-Y. Kim, W. F. Paxton, and J. F. Stoddart, *Org. Biomol. Chem.*, 2011, **9**, 2240–2250.